

A New Method of Preparing Embedment-free Sections for Transmission Electron Microscopy: Applications to the Cytoskeletal Framework and Other Three-dimensional Networks

DAVID G. CAPCO, GABRIELA KROCHMALNIC, and SHELDON PENMAN

Department of Biology, Massachusetts Institute of Technology, Cambridge, Massachusetts 02139. Dr.

Capco's present address is Department of Zoology, Arizona State University, Tempe, Arizona 85287.

ABSTRACT Diethylene glycol distearate is used as a removable embedding medium to produce embedment-free sections for transmission electron microscopy. The easily cut sections of this material float and form ribbons in a water-filled knife trough and exhibit interference colors that aid in the selection of sections of equal thickness. The images obtained with embedment-free sections are compared with those from the more conventional epoxy-embedded sections, and illustrate that embedding medium can obscure important biological structures, especially protein filament networks. The embedment-free section methodology is well suited for morphological studies of cytoskeletal preparations obtained by extraction of cells with nonionic detergent in cytoskeletal stabilizing medium. The embedment-free section also serves to bridge the very different images afforded by embedded sections and unembedded whole mounts.

Transmission electron microscopic (TEM)¹ images of conventional thin sections are influenced by the presence of the embedding material to a degree not often appreciated. The embedding resin, especially epoxy, scatters electrons very much the way the embedded specimen does, rendering it nearly invisible, except where heavy-metal stains are bound (9). The thin section is most effectively stained at its surface (11, 18) and is thus essentially a two-dimensional slice of three-dimensional objects whose actual morphology can only be reconstructed with difficulty. Such images formed from exceedingly thin planes are excellent for visualizing many biological structures but are inappropriate for examining three-dimensional networks of protein filaments (5) such as those constituting the cytoskeletal framework (i.e., surface lamina and a protein filament network surrounding the chromatin-containing nucleus: reference 13).

An alternate but under utilized method of electron microscopy, the unembedded whole mount, provides an image

directly from the specimen without resort to heavy-metal stains. In this procedure, the entire fixed, dehydrated, and critical-point dried cell is placed in the electron beam path *in vacuo* and biological material scatters electrons sufficiently to form very high contrast images. The important differences between stained, embedded sections and unstained whole mounts has been discussed in detail by Wolosewick and Porter (23, 24) for unextracted, fixed (i.e., intact) cells.

The embedment-free whole mount has proven essential to the study of the cell architecture remaining after cells have been extracted with nonionic detergent. This procedure removes most lipids and soluble components leaving the cytoskeletal framework (for reviews see references 13 and 14). This entity, revealed by detergent extraction, retains the configuration of the unextracted cell. Such preparations appear quite empty of structural elements when viewed in the TEM using epoxy-embedded thin sections. However, in the unembedded whole mount, the anastomosing three-dimensional network is visible (5).

The whole mount preparation has important technical limitations. The cell structures must be relatively thin and the filament networks sufficiently sparse for the images to be

¹ *Abbreviations used in this paper:* DGD, diethylene glycol distearate; MDCK, Madin-Darby canine kidney; nBA, *n*-butyl alcohol; TEM, transmission electron microscopy.

interpretable when the entire three-dimensional structure is viewed. Sometimes the geometry of cells and cell structures precludes the effective use of the cell whole mount. For example, most mitotic cells are rounded and consequently too thick to provide clear images of chromosomes and the cytoskeletal network. The nuclear-cytoplasmic borders of detergent-extracted cells are too dense to permit tracing the path of a single cytoskeletal or nuclear matrix filament (13). In addition, the familiar images of structures such as desmosomes, centrioles, and nuclear pores are based largely on the two-dimensional images produced by the epoxy-embedded thin sections which provide a view of the organelle in cross section. These objects are often unrecognizable when seen in three-dimensional whole mounts, which do not show the typical cross-sectional view. An unembedded section is required to bridge the difference between the two very different methods of imaging. The unembedded section methodology would (a) remove extraneous cell material from the object of interest and permit viewing in cross section, (b) result in sharp, high contrast images, (c) permit visualization of thicker sections (because in the absence of embedding medium, the electron beam could easily penetrate thicker specimens), and (d) display many three-dimensional aspects of the specimen.

We report the use of diethylene glycol distearate (DGD), $[\text{CH}_3(\text{CH}_2)_{16}\text{CO}_2\text{CH}_2]_2\text{O}$ as an embedding medium for obtaining easily handled thin or thick embedment-free sections for ultrastructural studies. This material has been used previously for light microscopy (1, 8, 17, 21, 22).

The unembedded section was pioneered by Wolosewick (25) using polyethylene glycol, but the DGD embedding material used here offers several significant advantages over the former medium. The advantages of the procedure described in this report are (a) the much reduced brittleness and consequent freedom from fracturing and crumbling when the block is cut, (b) that sections can float on the water-filled knife trough and ribbons of sections can be produced (this greatly eases the problems of handling), and (c) that sections produce interference colors allowing sections of equivalent thickness to be selected. The embedding medium is then removed without apparent damage to the biological material. In this report, we describe the application of the procedure to the morphological study of the detergent-extracted interphase and mitotic cells.

MATERIALS AND METHODS

Cell Culture: Suspension culture HeLa cells (CCL 2.2) were grown in spinner bottles in Eagle's minimal essential medium supplemented with 7% horse serum. Madin-Darby canine kidney (MDCK) cells, which form an epithelial-like sheet in culture (16), were grown in Dulbecco's modified Eagle's medium supplement with 10% fetal calf serum.

Collagen and Agar Preparation: The collagen gel was prepared by neutralizing an acidic solution of collagen to a final concentration of ~ 1.5 mg/ml and warming to 37°C. The agar gels were prepared by solubilizing agar to 2% in water at 100°C and allowing drops of the solution to cool on coverslips. Both were fixed and processed as the cells (described below).

Cell Preparation and Embedding in DGD: The anchored MDCK cells grown on glass Petri plates were processed in situ through extraction, fixation, and embedding (described below).

Suspension-grown HeLa cells were usually pelleted and the pellet was processed through the various solutions. Alternatively, both intact and detergent-extracted cells were processed through fixation, dehydration, and embedding by pouring the HeLa cell suspension into bags composed of four layers of lens paper (Kodak, Rochester, NY). The lens paper bags act as a filter, retaining most of the cells and allowing the solution to pass through. Once these bags are in an ethanolic solution, they are stable to disruption.

Intact cells were washed in PBS (4°C) and either fixed directly (described below) to examine the unextracted cells or first detergent extracted at 4°C (5) to produce the cytoskeleton. Cells were extracted with detergent in cytoskeletal buffer (100 mM NaCl, 10 mM PIPES buffer [pH 6.8], 3 mM MgCl_2 , 300 mM sucrose, 1.2 mM phenylmethyl sulfonyl fluoride, 0.5% Triton X-100) at 4°C. The anchored MDCK cells and the suspended HeLa cells were exposed to the extraction buffer for a time period which allowed complete removal of the cell's soluble components (for MDCK cells 10 min; for HeLa cells, 3 min). The intact and detergent-extracted cells were fixed in 2% glutaraldehyde in cytoskeletal buffer for 30 min at 4°C. The cells were washed three times with 0.1 M sodium cacodylate buffer, pH 7.2, (10 min each wash). The cells were postfixed with 1% OsO_4 in sodium cacodylate buffer 0.1 M for 5 min at 4°C and subsequently washed in 0.1 M sodium cacodylate. Alternatively, some of the extracted HeLa cells processed through the bag method were not postfixed (to prevent the bag disruption). Postfixation with OsO_4 is not necessary for the contrast of a TEM image since the image is formed directly by electron scattering of the biological material. Rather it serves as an additional fixative and as a stabilizer for the specimen in the electron beam. Careful comparison showed no detectable difference in the images of specimens with and without OsO_4 aside from the greater stability of samples lightly fixed with OsO_4 .

The cells were dehydrated through a series of increasing ethanol concentrations ending with three changes of 100% ethanol for 1 h each. Since DGD (Polysciences, Inc., Warrington, PA) is not soluble in ethanol, a transition fluid is required. Although DGD is soluble in toluene, a standard transition fluid in wax embedment procedures (7), the preferred solvent is *n*-butyl alcohol (nBA) which seems to afford a slightly better preservation of thin filaments in sections. nBA has been used in other wax embedment procedures (7).

Subsequently, the cells were immersed in a mixture of nBA/ethanol of 2:1 and then 1:2, followed by four changes of nBA for 15 min each. Because DGD is a solid at room temperature, it was maintained at 60°C to keep it molten during the embedding procedure. The cells were transferred from 100% nBA to DGD through a series of nBA/DGD mixtures of 2:1 and then 1:2, at 60°C, 10 min each, followed by three changes of 100% DGD for 1 h each. Cells anchored on glass Petri plates were removed from the oven and the DGD was allowed to harden. The glass Petri plates were then shattered with a hammer to separate DGD-embedded cells from the glass. Small fragments of DGD containing the MDCK monolayer were cut and mounted on blocks for ultramicrotomy. Fragments of DGD-infiltrated HeLa cell pellet and, alternatively, the HeLa cells processed through DGD in lens paper bags (which were opened under an infra red heat lamp) were transferred to embedding molds filled with DGD which were then cooled at 23°C to allow the wax to harden.

Sectioning and Removal of DGD: The DGD blocks were cut using glass knives at an angle of 10° on an MT-2B Porter-Blum ultramicrotome. After sectioning, both thick and thin DGD sections were placed on parlodion-coated, carbon-stabilized grids coated with 0.1% poly-L-lysine to increase the section adherence. The section-containing grids were stored overnight in a desiccator. The DGD was then removed by immersing the grids in 100% nBA at 23°C. Thin DGD sections (gold interference color) required three 1-h changes of nBA to completely remove the wax. Thicker DGD sections (purple interference color) required longer times to remove the DGD with nBA. For sections of still greater thickness ($\geq 0.5 \mu\text{m}$), toluene was used instead (four 3-h changes of toluene at 23°C). The grids were returned to 100% ethanol through a graded series of transitional solvent ethanol mixtures, washed three times in 100% ethanol, and then dried through the CO_2 critical point. Sections were examined in a JEOL JEM 100B electron microscope at 80 kV. The collagen and agar specimens were processed as described, except that the detergent extraction was omitted.

Preparation of Cell Whole Mounts: Cell whole mounts were prepared as described previously (5). Cells were grown on gold grids and then detergent extracted, fixed, dehydrated, and critical-point dried.

Epon-Araldite Embedding: The cells were extracted, fixed, and dehydrated as described above, then infiltrated with the resin through a graded series of propylene oxide and plastic mixture followed by three changes (1 h each) of Epon-Araldite. The final infiltration with the epoxy mixture was done overnight. The specimens were placed in embedding molds containing fresh Epon-Araldite and allowed to polymerize in an oven at 60°C for 2 d. The collagen and agar specimens were prepared as described above, except that the detergent extraction was omitted. Thin sections (gold interference color) were cut on a MT-2B Porter-Blum ultramicrotome using glass knives. Sections were poststained with a 10% aqueous solution of uranyl acetate followed by Reynolds's (15) lead citrate.

Section Thickness Estimation: In reflected light, DGD sections produce a series of interference colors on water of the knife trough; from thinnest to thickest, the colors are gold, purple, and blue. We estimated the section thickness of gold and purple interference sections as follows:

Wax sections of a given interference color were placed on grids or glass

FIGURE 1 Comparison between TEM images of epoxy sections and embedment-free sections of collagen and agar gels. All sections produced a gold interference color at the time of sectioning. The Epon-Araldite sections were poststained with uranyl acetate and lead citrate. The embedding medium was removed from the DGD sections as described in Materials and Methods. A collagen gel was prepared and fixed as described in Materials and Methods and embedded in Epon-Araldite (a) or DGD (b). The epoxy-embedded section (a) contains many short filament segments and dots (representing filaments sectioned near to perpendicular) while the embedment-free collagen section (b) shows an interconnecting filament network. A 2% agar gel prepared and fixed as described in Materials and Methods was embedded in Epon-Araldite (c) or DGD (d). These comparisons indicate that embedment-free sections (b and d) produce a high contrast image that does not require heavy-metal stains. In contrast, epoxy-embedded sections of agar (c) afford no visualization of the specimen since the polysaccharide does not stain with heavy metals. (a-d) $\times 10,000$.

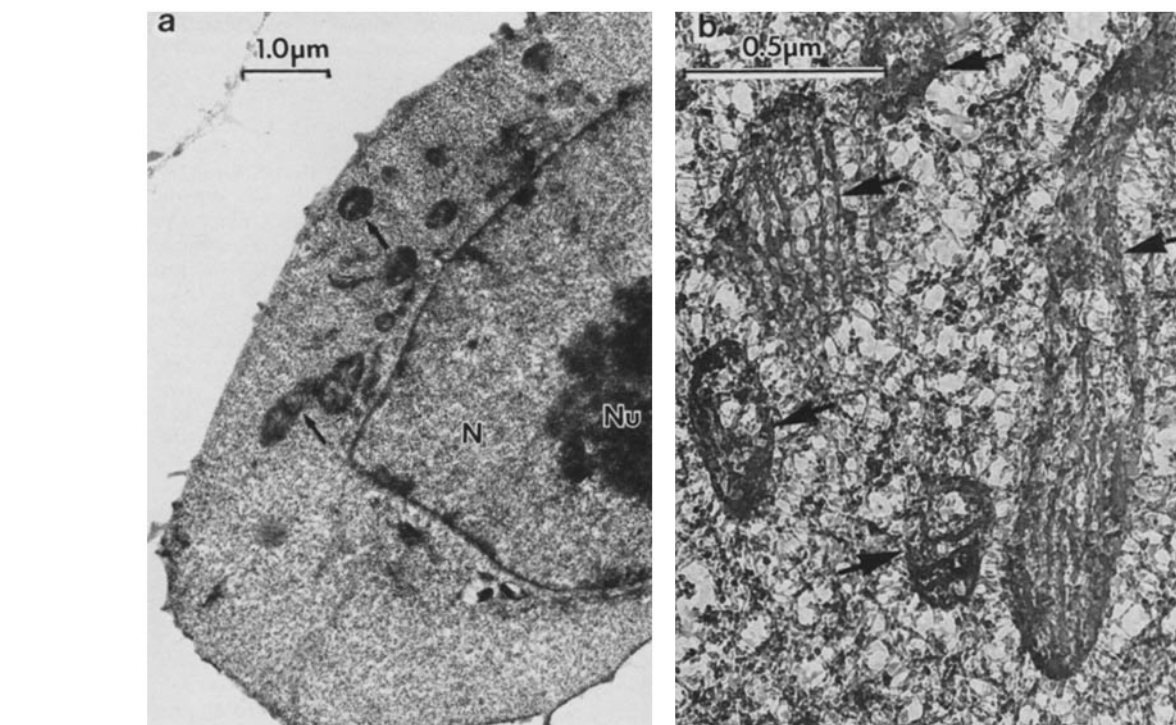
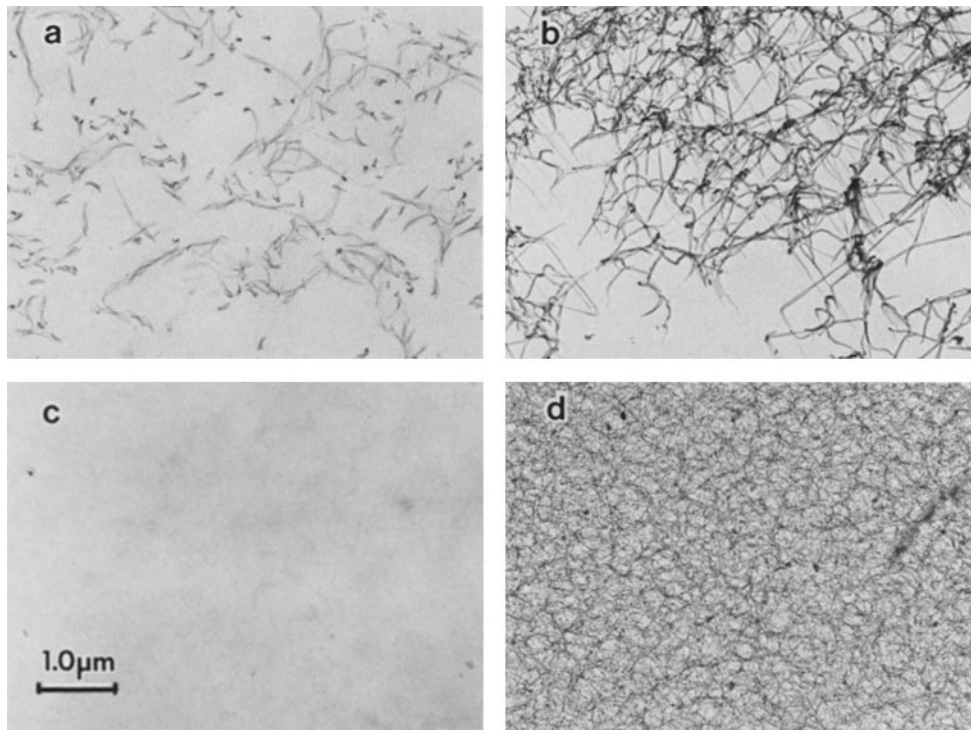


FIGURE 2 TEM image of an embedment-free section of an unextracted HeLa cell. Cells were washed in PBS (4°C), sedimented into a pellet, fixed with 2% glutaraldehyde in 0.1 M sodium cacodylate (30 min, 4°C), and washed, and then poststained in 1% OsO₄ in 0.1 M sodium cacodylate, embedded in DGD, and sectioned to produce a gold interference color. Embedding medium was removed as described in Materials and Methods. The image of the intact HeLa cell (a) is similar to those described by Wolosewick (25) in tissue using polyethylene glycol. A nucleolus (Nu) can be observed in the nucleus (N). The cytoplasmic region contains mitochondria (arrows) and microvilli are visible at the cell periphery. $\times 11,000$. (b) The high power micrograph of an unextracted HeLa cell shows the cytoplasm matrix with the microtrabecular lattice. Mitochondria (arrows) with cristae are clearly identified. $\times 53,000$.

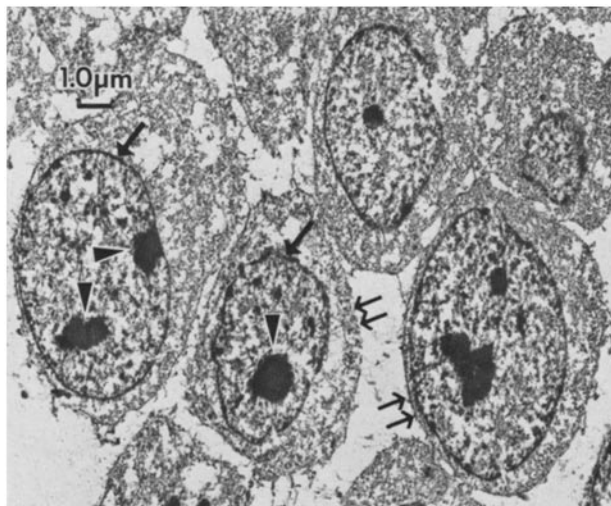
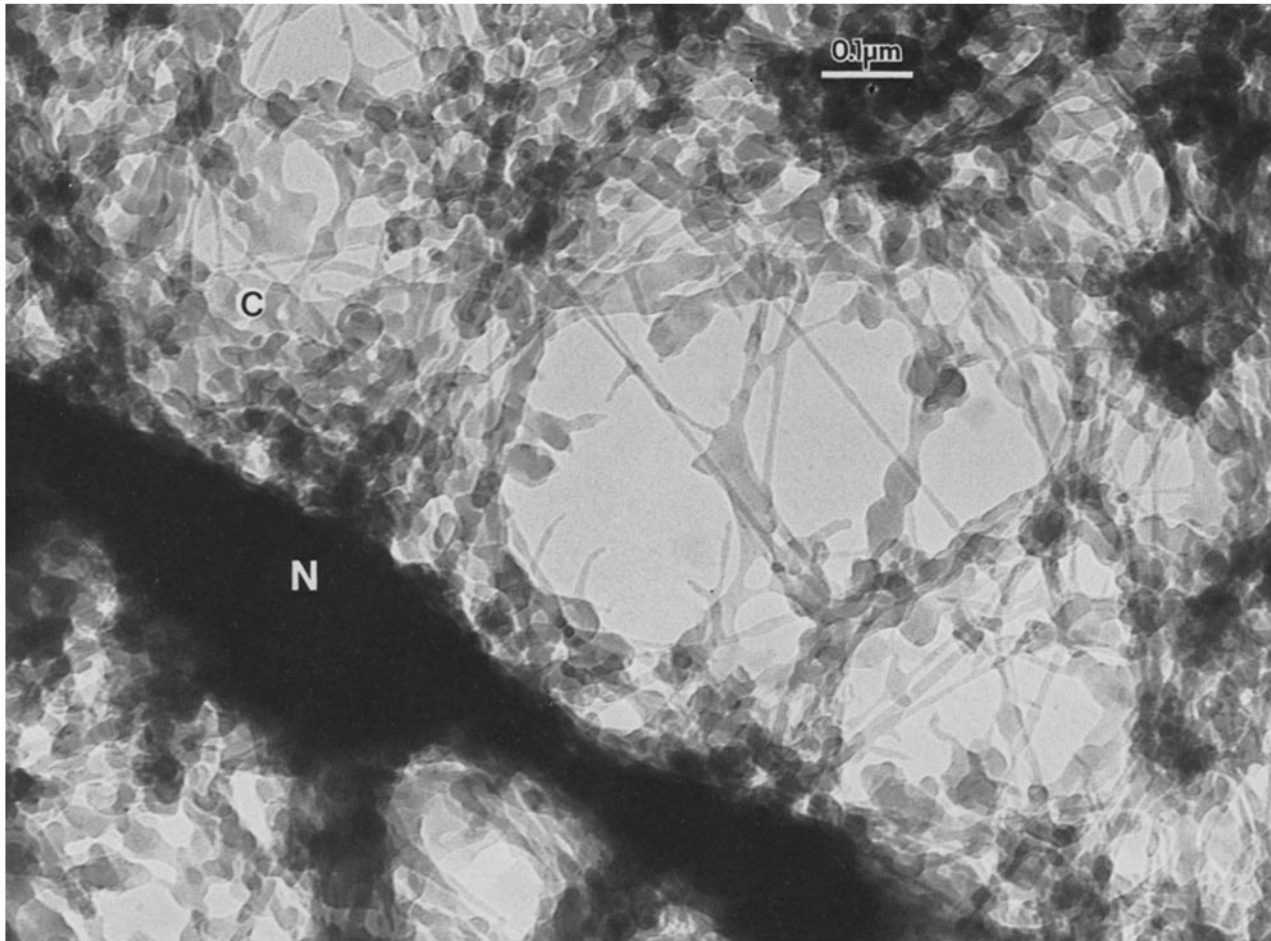


FIGURE 3 DGD embedding-free section of detergent-extracted HeLa cells. The embedding medium was removed as described in Materials and Methods. (bottom) A typical survey view of a thin section (gold interference color) through detergent-extracted HeLa cells. Some of the empty spaces within the cells are the result of producing thin sections through a filament network from which embedding medium is then removed (some unlinked filament segments are lost; see text). The nucleoli (arrowheads), nucleus (arrows), plasma lamina (double arrows), and internal cytoskeleton are visible. $\times 3,500$. (top) Thick embedding-free section (purple interference color) of the nucleocytoplasmic border. The chromatin-containing nucleus is visible on the left (N) and the cytoskeleton (C) composed of a fine filament network is shown on the right. $\times 120,000$.

coverslips, and then latex beads of known sizes were applied and dried onto the coverslips. The specimens were then coated with 12 nm of gold/palladium and examined in a scanning electron microscope (ISI DS 130) at a tilt angle of 80° (stereo micrographs were made). The height of the latex beads was compared with the height of the section in order to estimate the section thickness. Gold interference color sections are 100–200 nm thick and purple interference color sections are 200–400 nm thick.

RESULTS

A comparison of the images produced from embedded and poststained sections and images of embedding-free, unstained sections is shown in Fig. 1. A collagen gel was pre-

pared, cut into small blocks, and fixed with glutaraldehyde and osmium tetroxide. The blocks were dehydrated with ethanol and infiltrated with Epon-Araldite or DGD, as described in Materials and Methods. Gold interference color sections were cut from the epoxy-embedded sample, placed on grids, poststained with uranyl acetate and lead citrate, and viewed by TEM. Gold interference color sections were cut from the DGD-embedded material and collected on grids, and then the embedding medium was removed and the sections were processed for electron microscopy as described in Materials and Methods.

The epoxy-embedded section (Fig. 1*a*) shows separate, unconnected filaments and numerous black dots, presumably due to filaments at grazing incidence to the section surface and those intersecting the section obliquely, respectively. In contrast, the DGD preparation (Fig. 1*b*) shows a sharp, high contrast image of an interconnected filament network, as is characteristic of a gel. Fig. 1, *c* and *d* shows sections of a 2% agar gel prepared as described for the collagen gel. Essentially no structure is visible in the epoxy section (Fig. 1*c*), though care was taken to insure that a sample was present. Presumably, the heavy-metal stains used have little affinity for the polysaccharide polymers of the agar gel and thus do not enhance the image. In contrast, the DGD section (Fig. 1*d*) shows the polymer network with great clarity, demonstrating again the formation of a high contrast electron microscopic image without the heavy-metal stains. These results point to the utility of embedment-free sections in the analysis of biological specimens.

The TEM images obtained with DGD as an embedding medium are identical to polyethylene glycol sections when intact (i.e., unextracted) HeLa cells are examined. Fig. 2, *a* and *b* shows embedment-free sections of an unextracted HeLa cell prepared using DGD as the embedding material. The nucleus, nucleolus, microvilli, and membrane-bound organelles such as mitochondria are easily identified and the image can be compared with similar preparations shown by Wolosewick (25). The fine meshwork seen when the soluble proteins are not extracted, corresponding to the "microtubeculae" is shown in the higher magnification micrograph in Fig. 2*b*.

When cells were extracted with detergent, fixed, processed into DGD, and sectioned, and the embedding medium was removed (see Materials and Methods), the biological material produced high contrast images in the TEM (Fig. 3). Fig. 3, bottom, is a typical low magnification survey view of a section through suspension HeLa cells which produced a gold interference color at the time of sectioning. The chromatin-containing nucleus, the cytoskeleton, and remnant microvilli at the periphery of the cytoskeleton can be observed. Fig. 3, top, shows a higher magnification view of a thicker section (i.e., purple interference color) of a HeLa cell. When the embedding medium is removed, even relatively thick sections can be viewed with the penetrating power of an 80 kV electron beam. This figure illustrates the distinct filament network seen previously in detergent-extracted cell whole mounts (5).

The empty spaces encountered in very thin sections (i.e., gold interference color) illustrate a problem arising when relatively open filament networks are cut to a thinness comparable to the average spacing between filaments. Since the embedment-free section is attached to the grid by means of the filaments in contact with the supporting film, some filaments traversing the sections lose their points of attachment, and consequently, when the embedding material is removed, these free filaments are lost. This is a consequence of sectioning material from a fairly open network and then removing the supporting medium. The loss of material becomes less noticeable as the thickness of the section increases since the fraction of filaments with no attachment point in the section decreases.

Another view of the embedment-free section is afforded by the scanning electron micrograph in Fig. 4. This shows a thick section (purple interference color) of a detergent-extracted HeLa cell, after removal of DGD, critical-point drying,

and sputter-coating. The major structural features of the sectioned cell are apparent (i.e., the chromatin-containing nucleus and the plasma lamina). Moreover, no obvious rips or gouges resulting from knife damage are apparent. This sample is viewed at a 30° tilt and shows some of the plasma lamina at its proximal edge. In addition, the critical-point dried embedment-free section has not collapsed onto the surface of the grid.

A comparison of the images obtained from an epithelial colony (MDCK) using an epoxy thin section, an unembedded whole mount, and an embedment-free section are shown in Fig. 5. Cells were detergent-extracted and prepared for TEM as described in Materials and Methods. Equivalent regions of an MDCK colony are shown at the same magnification. The colonies were sectioned parallel to the culture dish surface so that the direction of viewing is equivalent in the three samples. The epoxy thin section in Fig. 5*a* shows well preserved junctional complexes, but cell interiors show only a random array of dots and some filament segments surrounding a nucleus. There is little to suggest any organization of the detergent-resistant cytoskeleton. The whole mount in Fig. 5*b* shows the existence and organization of the filament network, but details cannot be observed because too many filaments are superimposed (this results from the three-dimensional, columnar cell shape viewed in two-dimension on the photographic plate). The embedment-free section, Fig. 5*c*, shows the nucleus with nucleoli (indistinguishable in the whole mount). The cytoskeletal filaments are seen as an anastomosing network throughout the cell interior and in a prominent

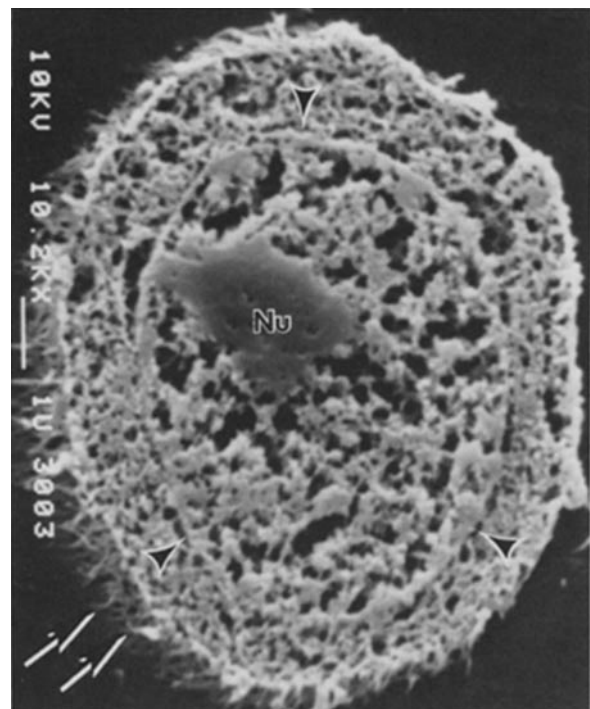


FIGURE 4 Scanning electron micrograph of a DGD embedment-free section of detergent-extracted HeLa cell. After removal of embedding medium, this thick section (purple interference color) was sputter-coated with 12 nm of gold-palladium. The sample was viewed at 30° tilt to allow the observation of the surface lamina (arrows) which is still intact after sectioning. The nucleolus (*Nu*), nucleus (arrowheads), and the cytoskeletal framework are clearly seen. The image also shows the uniform thickness of the section. $\times 10,000$.

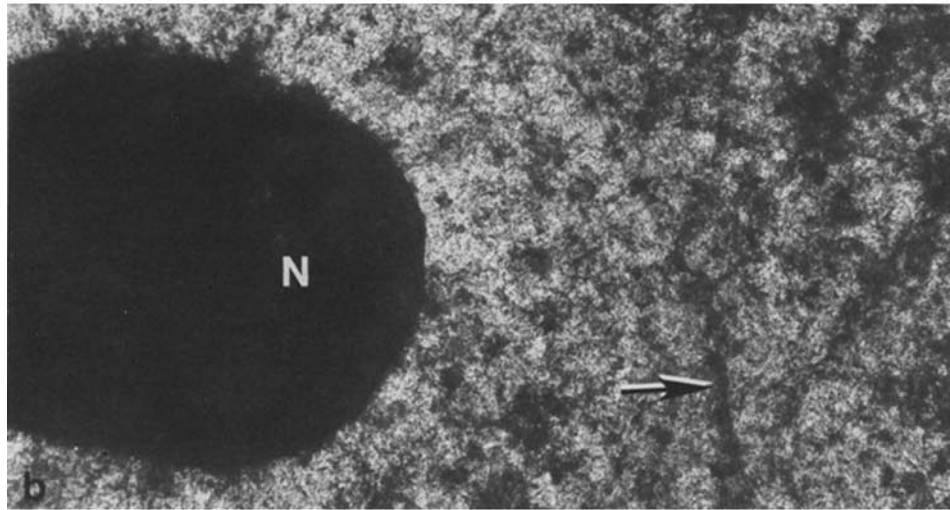
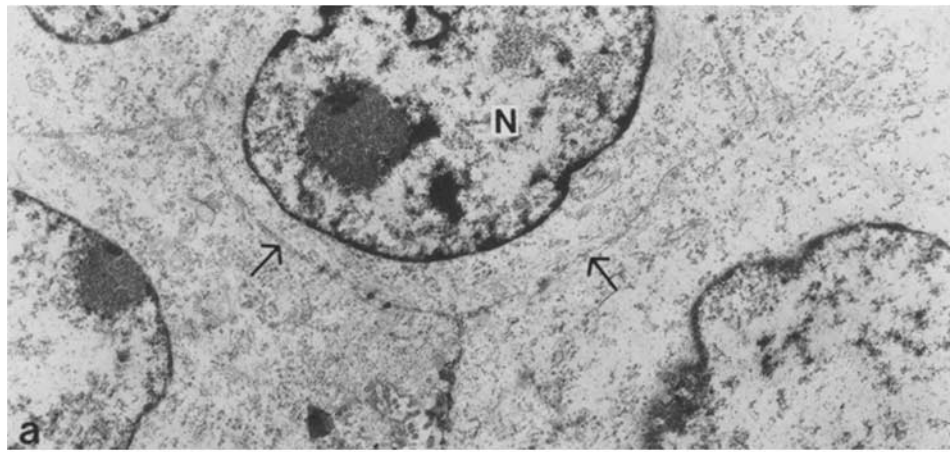


FIGURE 5 TEM images of (a) epoxy-embedded thin section, (b) unembedded whole mount, and (c) embedded-free section of detergent extracted MDCK cells. MDCK cells were sectioned parallel to the substrate to afford a direction of viewing similar to that of the whole mount. This section is through the apical part of the colony and thus the ovoid nuclei (N) are not at their maximum diameter, as is indicated in the unembedded whole mount. In the epoxy-embedded specimen (a), the cytoplasm appears to contain little material with no spatial organization. While the unembedded whole mount (b) demonstrates the existence of the cytoplasmic network, the thickness of the cell precludes analysis of the spatial pattern of individual filaments. The embedment-free section (c) allows observation of the filaments' spatial organization. Filaments run parallel to the cell-cell border (arrows). The interior of the nucleus is now visible, which is not the case with the unembedded whole mount. (a-c) $\times 8,000$.

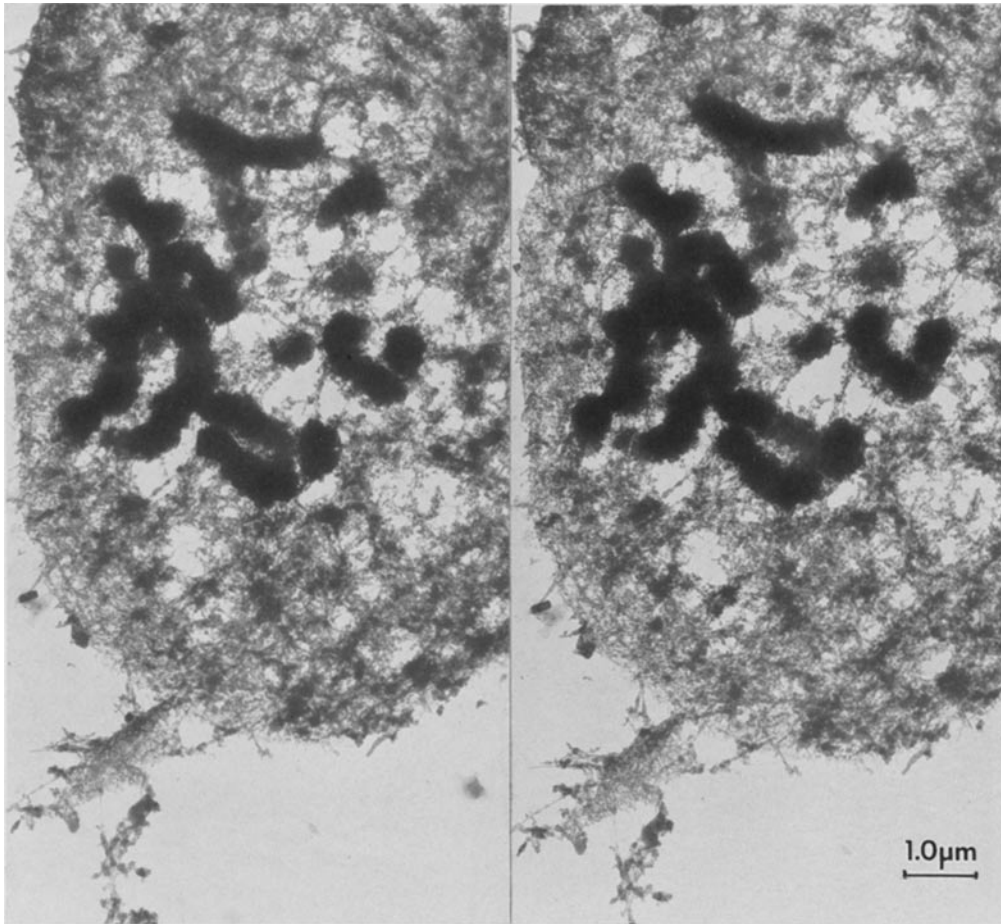


FIGURE 6 Stereopair electron micrograph of embedding-free section of a detergent-extracted mitotic HeLa cell. Microtubules have been depleted by cold treatment during extraction. In the unembedded whole mount, cell thickness precludes this view. In stereo, the embedding-free section shows the cytoskeletal framework interacting with chromosomes at various points along their length. $\times 9,000$.

bundle parallel to the cell-cell border.

The utility of the embedding-free section is best shown when applied to material that cannot be viewed in a whole mount preparation. One example is the skeletal framework of the mitotic cell, which in most cases is too thick and dense for whole mount electron microscopy. Whole mount electron micrographs of detergent-extracted mitotic PTK₂ cells have been obtained since these cells round up to a lesser extent than most, but even in this case, visualization of the filament network in association with the chromosomes was limited by cell thickness (6).

The embedding-free thick section (i.e., purple interference color) of a detergent-extracted mitotic HeLa cell is shown in the stereo TEM micrograph of Fig. 6. Microtubule elements of the mitotic apparatus have been depleted by cold treatment before and during extraction. This permits a clearer image of the chromosomes and associated filaments since the view is not obstructed by the microtubules. The chromosomes can be observed in contact with elements of the cell's filament network throughout their length. In addition, the stereo view demonstrates that the section has not collapsed onto the surface of the grid.

DISCUSSION

A simple and easily managed procedure for producing sections of cell material free of embedding medium has been developed using diethylene glycol distearate (DGD). The methodology is particularly suited for the detergent-extracted

cell preparations that are now used more routinely. There appears to be good preservation of cell structure even when the sectioned material is relatively empty and fragile, as is the case with the cytoskeletal framework. The comparison between epoxy and DGD sections also shows that the embedding plastic obscures much of the filament three-dimensional structure of the cytoskeletal framework and this accounts for the apparent discrepancy between the images from whole mount electron microscopy of extracted cells and those from conventional thin sections of the same material. The greatest utility of embedding-free sections is realized when they are viewed by stereo microscopy.

The cytoskeletal framework of detergent-extracted cells is essentially an empty structure consisting mostly of space-filling filament networks. For this reason, the penetrating power of the standard 80-kV electron beam is more than adequate and the need for a high voltage electron microscope is obviated with the embedding-free section. Identical detergent-extracted structures have been examined by Heuser and Kirschner (10) using quick freeze, deep-etch technique with very similar results.

The embedding-free section characteristics permit examination of previously inaccessible material such as the border between the nuclear interior and the cytoplasmic filaments. Also, the ultrastructure of very thick material, such as mitotic cells, cuboidal, and columnar epithelia, can be viewed with all the advantages of an embedding-free specimens and with a resolving power possible from relatively thin

sections. Applications of this methodology to in situ hybridization (2, 4, 19), in situ translation (3) of mRNA in sections, immunolocalizations (12), and other techniques previously applicable only at the light microscopy level are now possible with the resolution afforded by the electron microscope.

We would like to thank David Commings of the Whitaker College EM Facility for valuable assistance with ISI DS 130 EM. We thank Pat Turner for preparation of this manuscript.

This work was supported by National Institutes of Health (NIH) grant number CA08416, and National Science Foundation (NSF) grant number 8004696-PCM, and NSF grant number 8309334-PCM. David G. Capco is an NIH (National Research Science Award) postdoctoral fellow.

Received for publication 9 November 1983, and in revised form 10 January 1984.

REFERENCES

- Cutler, O. I. 1935. Embedding of glycol stearate. *Arch. Pathol.* 20:445-446.
- Capco, D. G., and W. R. Jeffery. 1978. Differential distribution of poly(A)-containing RNA in the embryonic cells of *Oncopeltus fasciatus*. Analysis by *in situ* hybridization with a (³H)-poly(U)probe. *Dev. Biol.* 67:137-151.
- Capco, D. G., and H. Jäckle. 1982. Localized protein synthesis during oogenesis of *Xenopus laevis*. Analysis by *in situ* translation. *Dev. Biol.* 94:41-50.
- Capco, D. G., and W. R. Jeffery. 1982. Transient localizations of messenger RNA in *Xenopus laevis* oocytes. *Dev. Biol.* 89:1-12.
- Capco, D. G., K. M. Wan, and S. Penman. 1982. The nuclear matrix: three-dimensional architecture and protein composition. *Cell.* 29:847-858.
- Capco, D. G., and S. Penman. 1983. Mitotic architecture of the cell: the filament networks of the nucleus and cytoplasm. *J. Cell Biol.* 96:896-906.
- Galigher, A. E., and E. N. Kozloff. 1971. *Essentials of Practical Microtechnique*. Lea & Febiger, New York.
- Graham, E. T. 1982. Improved diethylene glycol distearate embedding wax. *Stain Technol.* 57:39-43.
- Guatelli, J. C., K. R. Porter, K. L. Anderson, and D. P. Boggs. 1982. Ultrastructure of the cytoplasmic and nuclear matrices of human lymphocytes observed using high voltage electron microscopy of embedment-free sections. *Biol. Cell* 43:69-80.
- Heuser, J. E. and M. W. Kirschner. 1980. Filament organization revealed in platinum replicas of freeze-dried cytoskeletons. *J. Cell Biol.* 86:212-234.
- Meek, G. A. 1976. *Practical Electron Microscopy for Biologists*. John Wiley and Sons, New York. 446.
- Pardue, R. L., R. C. Brady, G. W. Perry, and J. R. Dedman. 1983. Production of monoclonal antibodies against calmodulin by *in vitro* immunization of spleen cells. *J. Cell Biol.* 96:1149-1154.
- Penman, S., D. G. Capco, E. G. Fey, P. Chatterjee, T. Reiter, S. Ermisch, and K. M. Wan. 1983. The three-dimensional structural networks of the cytoplasm and nucleus. In *Spatial Organization of Eukaryotic Cells*. J. R. McIntosh, editor. *Modern Cell Biology Series*. Alan R. Liss, Inc., New York. 385-415.
- Penman, S., A. Fulton, D. Capco, A. Ben-Ze-ev, S. Wittelsberger, and C. T. Fyne. 1981. Cytoplasmic and nuclear architecture in cells and tissues: form, function, and mode of assembly. *Cold Spring Harbor Symp. Quant. Biol.* 46:1013-1028.
- Reynolds, E. S. 1963. The use of lead citrate at high pH as an electron-opaque stain in electron microscopy. *J. Cell Biol.* 17:208-213.
- Rindler, M. J., L. M. Chuman, L. Shaffer, and M. H. Saier. 1979. Retention of differentiated properties in an established dog kidney epithelial cell line (MDCK). *J. Cell Biol.* 81:635-648.
- Salazar, H. 1964. Diethylene glycol distearate embedding and ultramicrotome sectioning for light microscopy. *Stain Technol.* 39:13-17.
- Shalla, T. A., T. W. Carroll, and G. A. DeZoeten. 1964. Penetration of stain into ultrathin sections of tobacco mosaic virus. *Stain Technol.* 39:257-265.
- Singer, R. H., and D. C. Ward. 1982. Actin gene expression visualized in chicken muscle tissue culture by using *in situ* hybridization with a biotinated nucleotide analog. *Proc. Natl. Acad. Sci. USA* 79:7331-7335.
- Sjöstrand, F. S. 1968. *Electron Microscopy of Cells and Tissues*. Academic Press, Inc., NY. 298.
- Taleporos, P. 1974. Diethylene glycol distearate as an embedding medium for high resolution light microscopy. *J. Histochem. Cytochem.* 22:29-34.
- Taleporos, P. 1976. The composition and cutting properties of diethylene glycol distearate from various sources. *J. Histochem. Cytochem.* 24:1285-1286.
- Wolosewick, J. J., and K. R. Porter. 1976. Stereo high-voltage electron microscopy of whole cells of the human diploid line, WI-38. *Am. J. Anat.* 147:303-324.
- Wolosewick, J. J., and K. R. Porter. 1979. Microtrabecular lattice of the ground cytoplasmic substance: artifact or reality. *J. Cell Biol.* 82:114-139.
- Wolosewick, J. 1980. The application of polyethylene glycol (PEG) to electron microscopy. *J. Cell Biol.* 86:675-681.